

31 p.

NASA TECHNICAL NOTE



N 63 20 888

CODE-1

NASA TN D-1705

NASA TN D-1705

OTS: \$ 0.75

PRELIMINARY INVESTIGATION OF PARTICLE-SUBSTRATE BONDING OF PLASMA-SPRAYED MATERIALS

*by Salvatore J. Grisaffe and William A. Spitzig;
Lewis Research Center,
Cleveland, Ohio*

*Washington, NASA
13 refs*

TECHNICAL NOTE D-1705

PRELIMINARY INVESTIGATION OF PARTICLE-SUBSTRATE
BONDING OF PLASMA-SPRAYED MATERIALS

By Salvatore J. Grisaffe and William A. Spitzig

Lewis Research Center
Cleveland, Ohio

NATIONAL AERONAUTICS AND SPACE ADMINISTRATION

NATIONAL AERONAUTICS AND SPACE ADMINISTRATION

TECHNICAL NOTE D-1705

PRELIMINARY INVESTIGATION OF PARTICLE-SUBSTRATE

BONDING OF PLASMA-SPRAYED MATERIALS

By Salvatore J. Grisaffe and William A. Spitzig

SUMMARY

An investigation was undertaken to evaluate the effects of two considerably different plasma spray powders, tungsten and zirconia, and four substrate materials, glass, stainless steel, tungsten, and copper, on the particle-to-substrate bond. All the substrates except glass were metallurgically polished; the glass had a sufficiently smooth surface so that mechanical interlocking would not contribute to the resultant bond.

It was found that the thermal conductivity of the substrate exerts the greatest control on the quench rate of the plasma-sprayed particles and, therefore, greatly influences the particle-to-substrate bond. In general, as the thermal conductivity of the substrate decreases, the quench rate of the particle decreases and particle adherence increases.

Although the properties of tungsten and zirconia are very different, the adherence of both materials, when sprayed in air, is very similar for any one substrate material (except in the case of a stainless-steel substrate where tungsten adherence was much better than that of zirconia). In a nitrogen atmosphere, tungsten adherence was the same as that observed in air, while there was a slight improvement in the adherence of zirconia.

INTRODUCTION

Although plasma spraying is becoming a common term in both industry and research, little work has been done to characterize the deposition sequence in order to obtain insight into the bonding phenomenon. It was felt, therefore, that a need existed for an examination of the particles that form the initial layer on the substrate. The purpose of this investigation was to evaluate the effects of two plasma spray powders and various substrate materials on the particle-to-substrate bond.

Earlier investigations dealing with the spraying process were not primarily concerned with the adhesion of individual particles to the substrate (refs. 1 and 2). In these investigations, the impact behavior of alumina particles with glass slides was studied, and the results were used to determine an optimum spray distance for the particular spraying operation.

. FACTORS THAT AFFECT PARTICLE-TO-SUBSTRATE BONDING

The quality of any sprayed coating is extremely dependent on the initial particle-to-substrate bond, and the actual bond strength will be influenced by the deposition conditions and the material properties. The actual configuration of a particle after it impinges and sticks to the substrate is dependent on many factors. Some of these are

(1) Particle factors

- (a) Temperature
- (b) Velocity
- (c) Mass
- (d) Density
- (e) Thermal conductivity
- (f) Specific heat
- (g) Thermal expansion
- (h) Dynamic viscosity
- (i) Surface tension

(2) Substrate factors

- (a) Temperature
- (b) Hardness
- (c) Surface finish
- (d) Thermal conductivity
- (e) Specific heat
- (f) Thermal expansion

(3) Plasma factors

- (a) Temperature
- (b) Velocity
- (c) Composition

The preceding factors also interact to influence other properties that contribute to the particle-substrate bond, and some of these are discussed in the

following paragraphs.

Total area of contact of particle against total area available for contact. - The deformed particles contact the substrate over a certain area, so any bond strength will be a function of the amount of interface area. For example, a first layer of particles that are relatively undeformed would give a low contact area, whereas one of highly deformed particles would cover much more of the available area.

The final particle shape is controlled by particle viscosity, particle velocity and mass (i.e., kinetic energy), and particle surface tension on the substrate. Substrate thermal conductivity, temperature, and specific heat will control the length of time after impact that the particle remains in a state where viscous flow may occur.

Interfacial stress. - The initial temperature of the particle, as it contacts the substrate, and the thermal properties of the particle and the substrate coupled with their coefficients of thermal expansion will influence the particle quench rate and the resultant interfacial stress on final cooldown. Of course, the ability of both to undergo plastic deformation under this stress is also important.

Surface films. - Surface oxides or contaminants in general on either the substrate or the particle could enhance or inhibit strong particle-to-substrate bonds.

Interdiffusion. - The formation of a nonbrittle diffusion zone between the substrate and the first sprayed layer would be highly desirable because it would greatly improve the quality of the interfacial bond. The diffusion phenomenon is, of course, dependent on the compositional, thermal, and crystallographic properties of both materials.

Consideration and Selection of Materials

During plasma spraying, powder particles originally at room temperature are first heated at a very rapid rate when they are blown into the plasma stream by a carrier gas. At this same time, they are physically accelerated to a relatively high velocity, which then decreases with increasing distance from the nozzle. They are then carried downstream by the flowing plasma to some point at which they collide with a substrate and are deposited. Such particles lose heat by radiation and convection as they move in the stream and, upon impact with the substrate, are further cooled by conduction.

Because each powder particle undergoes this process, it is easily seen that the scope of each step (at constant torch conditions) is governed by the physical properties of the powder being sprayed and the substrate on which it is deposited:

(1) Thermal conductivity, surface area, particle size, emittance, and specific heat govern how fast the particles both gain and lose thermal energy.

(2) Particle size and density govern to what velocity a particle is accelerated by the plasma and also how fast it decelerates.

(3) The thermal conductivity of the substrate, along with substrate temperature, determines how rapidly the particles lose heat on impact.

It appears, therefore, that the thermal conductivities of both substrate and powder are important variables.

Plasma spray powders and substrate materials that had considerable differences in their properties were chosen, in order to evaluate the effect of property variation on the particle-substrate bond. As many of the nonmaterial variables (e.g., plasma variables) as possible were held constant in order to examine the material aspects of the powders and substrates more critically.

The spray powders used in this investigation were tungsten and zirconia. These powders were chosen because of their wide differences in the properties (e.g., thermal diffusivity, emittance, etc.) that influence particle bonding. For substrate materials, glass, stainless steel, tungsten, and copper were chosen primarily because of their wide variations in thermal conductivity.

The metal substrates were sprayed in air at torch-to-substrate distances of 3 to 7 inches and in a nitrogen atmosphere at a torch-to-substrate distance of 5 inches. The glass substrates were sprayed in air at a torch-to-substrate distance of 3 to 9 inches.

The Need for Temperature and Velocity Data

In order to characterize a process, it is desirable to be completely familiar with all its parameters. Since this investigation was concerned with hot particles impacting on substrates, it was desirable to know how hot the particles were and how fast they were traveling when they hit. Such information would aid considerably in the analysis of the resulting collisions. An attempt, therefore, was made in this investigation to characterize these variables.

APPARATUS AND PROCEDURE

All spraying was accomplished with a rigidly mounted Thermal Dynamics F-40 torch operating at the following fixed conditions:

Spray nozzle inside diameter, in.	7/32
Current, amp	450
Voltage, v	60
Plasma-nitrogen flow rate, cu ft/hr ¹	80
Plasma-hydrogen flow rate, cu ft/hr ¹	10
Carrier-nitrogen flow rate, cu ft/hr ¹	10
Continental Coatings hopper setting	11.9

¹Standard cubic feet per hour.

Measurement of Particle Velocity

The average velocity of the powder particles was determined by a method similar to that used in determining the velocity of sprayed alumina particles in the investigation of reference 3. In this procedure the plasma spray is directed normal to two rotating disks lying one behind the other. The first disk has a 1/2-inch-wide radial slot, which allows particles to pass through the disk and deposit on a glass slide mounted on the second disk. The pattern of the powder particles formed on the second disk is displaced in relation to the slit in the first disk by an amount that depends on the angular velocity of the disks.

From the lateral displacement P (ft), the radial distance of the displacement from the center of the disk R (ft), the distance between the two disks A (ft), and the number of revolutions of the disks per minute N (rpm), the average particle velocity V (ft/sec) can be calculated by means of the following equation, easily derived from geometric considerations:

$$V = \frac{2\pi R N A}{60 P}$$

In this investigation, two circular metal disks, 16 inches in diameter, with a 1-inch separation, were mounted on a motor-driven shaft. The rotational speed of the disks was measured stroboscopically.

Measurement of Particle Temperature

The determination of the zirconia- and tungsten-particle deposition temperatures was carried out by means of thermocouples. Platinum - platinum-13-percent-rhodium thermocouples were fabricated with oversized junctions that were then hammered into thin, flat disks approximately 0.010 inch thick and 0.125 inch in diameter. This provided a large recording surface of very low heat capacity. A recorder with a millisecond response was used to monitor the temperature. Profiles of temperature against distance from the nozzle were made in the plasma gases with and without particles in the stream. With this thermocouple, it was impossible to determine temperatures closer than 4 inches from the nozzle since the upper limit of the thermocouple is 3000° F. At each position, spray was directed at the thermocouple until a temperature equilibrium was reached, usually after about 0.5 second. The coating that formed on the thermocouple was removed before each new distance measurement.

Substrate Preparation

The glass microscope slides were cleaned with acetone but otherwise were used as received. The metal substrate materials were cut or ground to size, mounted in self-curing exothermic plastic, and metallurgically polished to produce a scratch-free surface.

Spraying in Air

Glass microscope slides were inserted directly into a wooden block with milled slots spaced at 1/2-inch intervals. The metal substrates were left in the original polishing mounts. Each mounted specimen was fitted with a hose clamp to which a metal tab had been welded. These tabs were inserted into the milled slots in the wooden block.

The actual deposition on both types of substrates was accomplished by drawing the block, on which the specimens were mounted, through the plasma spray at approximately 1 foot per second. In this way, particles were deposited on the substrates in such a manner as to be readily examined with a metallograph.

Spraying in Nitrogen

A procedure similar to that used for spraying in air was employed for the spray work in an inert atmosphere. A water-cooled spray chamber was used; it was evacuated to a pressure of 20 microns and then backfilled with high-purity dry nitrogen. A metal sliding mechanism was employed instead of the wooden block, but, again, the specimens were moved in front of the plasma stream at approximately 1 foot per second.

MATERIALS

Powder

The zirconia powder was calcium oxide stabilized and had a particle-size range of 62 to 44 microns (-250 to +325 mesh). The as-received powder was somewhat angularly shaped and, when viewed at high magnification under polarized light, showed many transparent areas. After passing through the jet, the powder particles more closely approximated spheres.

The particle size of the tungsten powder ranged from 62 microns (-250 mesh) to 30 microns (no equivalent mesh size). In the as-received condition, it appeared to be composed of sintered chains of smaller particles. After passing through the jet, the particles were nearly spherical.

Substrates

Both glass and a series of metals were used as substrates. Glass (soda lime) microscope slides (1 by 3 in.) served as the low-thermal-conductivity substrates, while 1- by 1-inch squares of metal, all taken from the same sheet, were used for more highly conductive substrates. The metals chosen were commercial tungsten sheet, 304 stainless steel, and oxygen-free high-conductivity copper. All samples were approximately 1/8-inch thick.

Physical properties of both the powders and substrates are given in table I. These values, from literature sources, are provided only for comparison of relative properties and should not be interpreted to be the actual values of the

materials used.

RESULTS AND DISCUSSION

Velocity Measurements

The results of the velocimeter measurements of tungsten and zirconia particles are shown in figure 1. The average velocity of the tungsten particles decreased from 250 to 150 feet per second as the distance from the nozzle was increased from 3 to 11 inches. At distances of 3 and 5 inches, the velocity was nearly constant (i.e., 250 and 235 ft/sec, respectively). For the zirconia particles, the velocity decreased from 430 to 310 feet per second as the distance from the nozzle increased from 3 to 11 inches. At 3 and 5 inches, however, the velocity remained nearly constant at 430 feet per second. These data show that, over the range of distances investigated, the zirconia particles attained a velocity twice that of the tungsten particles.

The resulting velocity data, in conjunction with the particle size and density of the tungsten and zirconia powders, show that the ratio of the square of the velocity of zirconia to that of tungsten is approximately the same as the ratio of the density of tungsten to that of zirconia. The kinetic energies of both powders, therefore, were approximately equal in this case (appendix A).

Temperature Measurements

Temperature of zirconia and tungsten particles. - Since no data existed as to the particle temperatures during plasma spraying, an attempt was made to obtain approximate values of the average particle temperatures of zirconia and tungsten. The method used for this analysis was similar to that used in a previous investigation (ref. 4). Because the temperature measurements are, in effect, an integration of the temperature of many particles, the results are average values of particle temperature. These data are presented in figure 2. The data points from several trials all fall within the region shown in figure 2. The actual variation in the readings was not considered unusual in view of the method used. The data indicate, however, that the particles were at a slightly higher temperature than the plasma stream. The temperatures recorded when either the tungsten or zirconia particles were in the plasma stream were approximately the same.

Heat transfer in zirconia and tungsten particles. - It was desirable to evaluate the effect of powder size on the thermal characteristics of the zirconia and tungsten particles. This analysis was carried out by means of the equation for heat flow in a sphere as presented in reference 5. The equation and the assumptions involved, along with a sample calculation, are shown in appendix B. This analysis allows calculation of the ratio of the temperature of the interior portions of the particle to that at the surface as a function of the thermal properties of the material and the residence time of the particles in the plasma stream. Selecting the distances 3 and 5 inches as the most probable range of spray distance and taking the average velocity of the particles as that measured in this range yield the results shown in figure 3. The curves are calculated

from equation (B1) (appendix B) and were taken from reference 5.

The maximum velocity was chosen as the average value for the calculation of residence time since this would give the shortest time that the particle was in the plasma stream; therefore, the particle sizes recorded in figure 3 should be on the conservative side. The calculations showed that, in the case of tungsten, the temperature at the center of the particle could be the same as that on the surface for diameters up to 100 microns for the distances selected. In the case of zirconia, the larger particle sizes (60 microns) result in the center of the particles having a temperature of about seven-tenths that of the surface. These values for particle size are in fair agreement with those calculated in the investigation of reference 6.

It should be noted that the effects of cooling the particles by radiation and convection have been ignored in these calculations and that the plasma stream was assumed to have a constant temperature along its length. It was further assumed that the surface of the particles reached the plasma temperature instantaneously upon entering the plasma stream. In spite of these assumptions and the additional ones listed in appendix B, it is felt that the calculated results are sufficiently precise for the conclusions drawn from them.

Because of this complex interaction of heat-transfer and plasma-temperature effects, no definite conclusions can be drawn about the actual condition of the particles as they impact the substrate. If the surface temperature of the particles when they enter the plasma stream is assumed to reach the melting point of the material, however, the heat-transfer analysis indicates that, even in the case of zirconia, the particles should be in a state in which they can easily be deformed, and deformation results in a large area of contact between the particles and the substrate. That the temperatures of the particles approach their melting points at some point in the plasma stream has been evidenced by their spherical shape after they pass through the plasma jet (ref. 7). Since the plasma-stream temperature actually decreases with increasing distance as the particles are traveling in it, additional complexities arise that cannot be accounted for in the heat-transfer analysis. It was felt that the best way to analyze the complex interaction of the changing plasma-stream temperature and heat transfer of the particles was to examine the resultant deformed particles on the various substrates.

Glass Substrate

Velocities, temperatures, and schematic cross sections of zirconia particles that impinged on glass slides are given in table II. A typical flow pattern is shown in figure 4. This type of flow pattern is very similar to the splash patterns obtained when water droplets impinged on a surface (ref. 8).

As the distance from the gun increases (i.e., particle temperature and velocity decrease), the splash patterns change from the type for high-velocity droplets to the type for low-velocity droplets (ref. 8).

Since glass has a very low thermal conductivity, it would be expected that the particles impinging on it would retain their heat for a longer time than they

would on a substrate with high thermal conductivity. Data obtained at this laboratory (as yet unpublished) indicate that the particle deformation is complete in approximately 7×10^{-5} second after contact with the substrate. This type of deposition, when compared to that in the high-speed photographs of water droplets in reference 8, indicates that the surface tension of the particles is quite low and that the flow characteristics may be related to the viscous drag between the solid surface and the flowing drop. Also, since the number of stringers decreases with distance (and velocity decreases with distance), these may be a function of the velocity.

Tungsten deposits on glass exhibited a somewhat different characteristic. Schematic cross sections are shown in table III, and a photograph is shown in figure 5. The particles deformed into flat circular plates with slight circumferential asperities. When distance was increased (temperature and velocity were decreased), the amount of spreading decreased. At relatively large distances, the particles exhibited the development of columnar grains. Evidently, the particles cooled slowly enough to permit observation of this structure. It was visible because there was surface oxidation of the particles, in effect, a heat-tint etch.

By a comparison of the patterns of zirconia and tungsten on glass, it may be seen that zirconia particles splashed considerably more than tungsten particles. This increased flowability was enhanced by the higher velocity of zirconia as compared to tungsten, even though the kinetic energies were almost equal. It also appears that the lower ratio of surface to center temperature of the zirconia particles, as compared to tungsten, did not have any obvious influence on the resultant configurations.

Stainless-Steel Substrate

Some adherence of zirconia on stainless steel was seen at the 3-inch working distance. The amount, however, was not at all significant, and few whole particles could be seen (fig. 6). Most of the deposit was nothing more than random splashes from particles that had hit and subsequently fallen off. Some gouges and pits were also observed. At the greater spray distances, the amount of residue decreased and only pits could be seen.

The deposition of tungsten on stainless steel was excellent at all distances. Small basal stringers were apparent, and many of the particles exhibited an unusual rectangular configuration on their top surfaces. Almost every particle exhibited a surrounding dark splash that may well have been due to either a slight cloud or shell of tungsten or tungsten oxide surrounding it, which splashed out on impact (fig. 7).

The adherence of zirconia on stainless steel was much less than that exhibited by tungsten. Since the coefficient of expansion of zirconia is greater than that of tungsten, the tungsten maintained a much better bond. This could indicate that metal-to-metal bonds have a much greater chance of success than ceramic-to-metal bonds or that the ductility of the coating is an important factor. Actually, both of these points should be carefully considered.

Conversely, the zirconia-to-glass bond seemed better than the tungsten-to-glass bond. Then, too, the tungsten was oxidized on glass because of the extremely low thermal conductivity of this substrate. Perhaps, the stainless-steel conductivity was low enough to permit good bonding but high enough to cool the tungsten and prevent rapid oxidation.

It is also possible that the similarity of the particle and substrate materials is an important factor in bonding; that is, metal particles bond better to metal, and oxide particles bond better to oxides. The numerous parameters involved in the bonding (e.g., thermal conductivity, type of oxide film on substrate, similarity of particle and substrate material, etc.), however, make definite conclusions about the controlling factor contributing to this bond impossible.

Zirconia seemed to adhere to stainless steel better when it was sprayed in the nitrogen atmosphere (5-in. working distance). This may be easily attributed to the higher temperature of the stainless-steel substrate (the tank-atmosphere temperature rose to approximately 300° F before spraying). Tungsten sprayed on stainless steel in the tank (also at 5 in.) was very similar to that sprayed in air and bonded well.

Tungsten Substrate

Zirconia exhibited almost no adherence to tungsten substrates at any of the working distances investigated when sprayed in air. Only a few fragments remained on the tungsten. This indicates extreme atomization of the particles on impact due to the high conductivity of the substrate. The substrate was pocked by many particles that did not adhere upon impact (fig. 8).

Tungsten did not atomize on impact at any of the distances (3, 5, and 7 in.) but deformed and then fell off; the resultant splash patterns were outlined by a ring of either the oxide or finely condensed tungsten (fig. 9). At the center of each splash pattern, there appeared to be a depressed area, probably caused by the initial high deformation, which occurred when the particles first struck the substrate.

Because of the higher thermal conductivity of the substrate, neither of the two powders adhered to tungsten as well as they did to stainless steel or glass.

Zirconia sprayed on tungsten in an inert nitrogen atmosphere showed a slightly improved adherence over that which it had exhibited at any of the working distances in air. This can again be attributed to the increase in substrate temperature that decreased the effect of high substrate thermal conductivity by lowering the temperature differential on impact.

Tungsten sprayed on tungsten in nitrogen showed the same type of phenomenon as tungsten sprayed on tungsten in air. Less outlining of the places where particles impacted was noticeable in the nitrogen atmosphere than in air. This indicates that much of the shadowing was due to surface oxidation of the particles.

Copper Substrate

No zirconia adhered to copper at any of the distances investigated in air. The copper substrates were pitted by the zirconia at these distances because heat was rapidly removed from the impinging particles by the high-thermal-conductivity copper. From the shapes of these pits, it may be observed that not all particles were completely spherical at impact and that some deformed slightly and caused gouging. At the greater distance, only the large particles had sufficient energy to cause pitting, so the number of pits decreased with distance, whereas the pit size increased. A typical picture is shown in figure 10. If a sufficient number of pits occurred, the surface would be in effect "plasma blasted," and then mechanically bonded zirconia could be present.

Tungsten sprayed on copper showed no adherence. The particles were plastic enough so that they deformed on impact. Since the copper surface oxidized and because of the extremely short time that the particles were at temperature, these impacting particles fell off and left outlines (fig. 11).

The combined observations on the deposition of tungsten and zirconia particles on all the substrates are listed in table IV.

CONCLUSIONS

Analysis of the deposition behavior of tungsten and zirconia particles on the various substrates shows that certain trends are followed.

Substrate thermal conductivity exerts the greatest control on the quench rate of the plasma-sprayed particles and thus greatly influences the particle-to-substrate bond. In general, as the thermal conductivity of the substrate decreases, the quench rate of the particle decreases and particle adherence increases.

Tungsten particles, having a significant amount of plasticity, merely deform on the high-thermal-conductivity substrates and then fall off, since no bond is established; while zirconia, being a more brittle material, atomizes when it contacts this type of substrate.

Although the properties of tungsten and zirconia are widely different, the adherence of both materials, when sprayed in air, is very similar for any one substrate material (except in the case of a stainless-steel substrate where tungsten adherence is much better than that of zirconia). In a nitrogen atmosphere, tungsten adherence is the same as in air, while zirconia adherence shows slight improvement. It is not known if this improvement is due solely to the increased thermal conductivity of the substrate as a result of spraying in the heated environment.

Lewis Research Center
National Aeronautics and Space Administration
Cleveland, Ohio, June 13, 1963

APPENDIX A

KINETIC-ENERGY CALCULATIONS

The density of tungsten ρ_W is 19.3 grams per cubic centimeter, the average velocity is 240 feet per second (7320 cm/sec), and the mass of a spherical tungsten particle is

$$\frac{\rho_W \pi d^3}{6} = 10.1 d^3 \quad \text{g/cm}^3$$

where d is the particle diameter. The kinetic energy of the particle is, then,

$$KE_W = 270 \times 10^6 d^3 \quad \text{g/(cm)(sec)}^2$$

The density of the zirconia used in this investigation ρ_Z is 6.0 grams per cubic centimeter, the average velocity is 430 feet per second (13,100 cm/sec), and the mass of a spherical zirconia particle is

$$\frac{\rho_Z \pi d^3}{6} = 3.14 d^3 \quad \text{g/cm}^3$$

Thus, the kinetic energy of the particle is

$$KE_Z = 270 \times 10^6 d^3 \quad \text{g/(cm)(sec)}^2$$

The specific value for a 60-micron particle, for example, is

$$KE_W = KE_Z = 270 \times 10^6 \text{ g/(cm)(sec)}^2 \times (6 \times 10^{-3} \text{ cm})^3 = 58.4 \text{ (dynes)(cm)}$$

APPENDIX B

HEAT-TRANSFER ANALYSIS

The equation for heat transfer in a sphere with radius R , initially at zero temperature, which is instantaneously brought to some constant temperature T_s at the surface, can be expressed (ref. 5) as

$$\frac{T}{T_s} = \left[1 + \frac{2R}{\pi r} \sum_{n=1}^{\infty} \frac{(-1)^n}{n} \sin\left(\frac{n\pi r}{R}\right) \exp\left(-\frac{Kn^2\pi^2 t}{R^2}\right) \right] \quad (B1)$$

where

- T temperature of particle at radius r
- T_s surface temperature of particle
- R radius of particle
- r distance from center to a point in the particle
- n integer
- K thermal diffusivity, $k/C\rho$
- t time of residence of particle in plasma stream
- k thermal conductivity
- C specific heat
- ρ density

Assumptions involved in the derivation of this equation as modified to apply to the case at hand are the following:

- (1) The plasma stream has a constant temperature along its length.
- (2) The powder particles are small spheres.
- (3) The thermal conductivity, specific heat, and density of the particles are independent of temperature.
- (4) The heat of fusion of the particles is zero, and the thermal conductivity, specific heat, and density are the same for the solid and liquid.
- (5) The particles are homogeneous and isotropic solids.

Sample Calculation of the Dimensionless

Term $kt/C_p R^2$ for Zirconia

The term $kt/C_p R^2$ is calculated by using the following values:

Thermal conductivity, k , Btu/(hr)(ft)(°F)	0.75
Specific heat, C , Btu/(lb)(°F)	0.170
Density, ρ , lb/cu ft	374
Particle radius, microns	30

At a 3-inch torch-to-work distance, the average velocity is 430 feet per second; the residence time is, therefore,

$$t = \frac{0.25 \text{ ft}}{430 \text{ ft/sec}} = 0.000582 \text{ sec}$$

Since

$$\frac{k}{C_p} = \frac{0.75 \text{ Btu/(hr)(ft)(°F)}}{0.170 \text{ Btu/(lb)(°F)} \times 374 \text{ lb/cu ft}} = 0.0118 \text{ sq ft/hr} = 0.00305 \text{ cm}^2/\text{sec}$$

then

$$\frac{kt}{C_p R^2} = 3.05 \times 10^{-3} \text{ cm}^2/\text{sec} \times 5.82 \times 10^{-4} \text{ sec} \times \frac{1}{(30 \times 10^{-4} \text{ cm})^2} = 0.20$$

REFERENCES

1. Moore, D. G.: Basic Studies of Particle-Impact Process for Applying Ceramic and Cermet Coatings. Nat. Bur. of Standards Repts. 6259, 6356, 6453, 6544, NBS, Oct. 1958 to Sept. 1959.
2. Meyer, H.: Das Verhalten von Pulvern im Plasmastrahl. Ber. Dtsch. Keram. Ges., bd. 39, H2, 1962, pp. 115-124.
3. Meyer, H.: Flame Spraying of Alumina. Library Trans. 943, British RAE, Apr. 1961.
4. Grisaffe, S. J.: A Preliminary Investigation of the Thermal History of Powder Particles During Plasma Spraying. Paper Presented at Fifth Refractory Composites Working Group Meeting, Dallas (Texas), Aug. 8-10, 1961.
5. Carslaw, H. S., and Jaeger, J. C.: Conduction of Heat in Solids. Second ed., Univ. Press (Oxford), Ch. IX, 1959.
6. Murphy, C. A., Poulos, N. E., and Walton, J. D.: Spray-On Refractory Coatings System Considerations. Paper Presented at Nat. Pyro-Metallurgical Program, AIME, Dallas (Texas), Feb. 1963.
7. Spitzig, W. A.: Sintering of Arc Plasma Sprayed Tungsten. M.S. Thesis, Case Inst. Tech., 1962.
8. Engel, O. G.: Waterdrop Collisions with Solid Surfaces. Jour. Res. Nat. Bur. Standards, vol. 54, no. 5, May 1955, pp. 281-298.
9. Lyman, Taylor, ed.: Metals Handbook. Vol. 1, Eighth ed., ASM, 1961.
10. Arne, V. L., and Wolfe, G. W.: Thermal Properties of Solids. CVA Rep. AST-E9R-12073, Vought Astronautics, Oct. 13, 1959.
11. Bradshaw, Wanda G., and Matthews, Clayton O.: Properties of Refractory Materials: Collected Data and References. IMSD-2466, Lockheed Aircraft Corp., Jan. 15, 1959.
12. Yavorsky, Paul J.: Properties and High Temperature Applications of Zirconium Oxide. Ceramic Age, vol. 78, June 1962, pp. 64-69.
13. Kingery, W. D.: Introduction to Ceramics. John Wiley & Sons, Inc., 1960.

TABLE I. - THERMAL PROPERTIES OF POWDERS AND SUBSTRATES

Material	Thermal conductivity near 68° F, (cal)(cm)/(cm ²)(sec)(°C)	Specific heat near 68° F, cal/(g)(°C)	Thermal expansion near 68° F, in./(in.)(°F)
Powders			
Tungsten	^a 0.397	^b 0.033	^a 2.55×10 ⁻⁶
Zirconia	^c .005	^b .10	^d 5.5×10 ⁻⁶
Substrates			
Glass	^e 0.004	^b 0.18	^b 4.52×10 ⁻⁶
304 Stainless steel	^a .039	^a .12	^a 9.9×10 ⁻⁶
Tungsten	^a .397	^b .033	^a 2.55×10 ⁻⁶
Copper	^a .941	^b .092	^a 9.2×10 ⁻⁶

^aRef. 9.^bRef. 10.^cRef. 11.^dRef. 12.^eRef. 13.

TABLE II. - PARTICLE VELOCITIES, TEMPERATURES, AND CROSS SECTIONS
OF ZIRCONIA PARTICLES SPRAYED ON GLASS

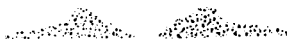
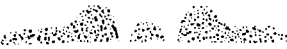

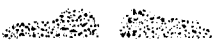
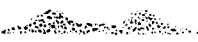
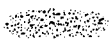

Spray distance, in.	Average particle velocity, ft/sec	Approximate particle temperature, °F	Schematic average particle cross section	Remarks
3	425	3300		Particle splashed away from center and developed a rather high circumferential rim from which stringers proceed outward. No material at center of impact.
4	430	2800		Small amount of material remains at center of impact, and ridge is separated from it by region of no material. Stringers still proceed radially outward, but ridge is on inside.
5	430	2300		Ridge is on inside, but stringer length and number have decreased markedly.
6	385	2000		Center hole is much smaller, the ridge much heavier, and the few stringers much shorter.
7	350	1800		The ridge remains, but no central hole exists. Stringers have degenerated into surface discontinuities.
8	330	1500		Particle is a distorted disk. A few flow lines can be seen.
9	320	1400		Almost no deformation occurred.

TABLE III. - PARTICLE VELOCITIES, TEMPERATURES, AND CROSS SECTIONS
OF TUNGSTEN PARTICLES SPRAYED ON GLASS










Spray distance, in.	Average particle velocity, ft/sec	Approximate particle temperature, °F	Schematic average particle cross section	Remarks
$1\frac{1}{2}$	---			Extreme flattening. Particle overlap. Heavy oxidation.
2	---			
3	250	3300		
4	245	2800		
5	235	2300		
6	225	2000		Columnar structure at particle center. May be due to slow cooling, is visible because of an effective heat tint from oxygen in atmosphere.
7	210	1800		
8	180	1500		
9	165	1400		

TABLE IV. - COMBINED OBSERVATIONS ON PARTICLES DEPOSITED ON SUBSTRATES

Substrate	Atmosphere	
	Air	Nitrogen
Glass	Tungsten adhered at all distances but oxidized heavily because of slow cooling (fig. 5).	-----
	Zirconia adhered well at all distances and exhibited random cracks in all particles (fig. 4).	-----
304 Stainless steel	Excellent adherence of tungsten at all distances. Some particles were surrounded by dark splashes and many showed square tops (fig. 7).	Same as in air.
	Zirconia particles atomized, and only small fragments adhered (fig. 6).	Slightly better adherence, but the deposition configurations were the same.
Tungsten	Tungsten particles hit and fell off (fig. 9).	Same as in air.
	Very little adherence of zirconia particles and much atomization (fig. 8).	Slightly increased adherence of fine particles.
Oxygen-free high-conductivity copper	Tungsten particles hit and fell off (fig. 11).	Same as in air.
	Zirconia pitted the substrate but did not adhere (fig. 10).	Slight adherence.

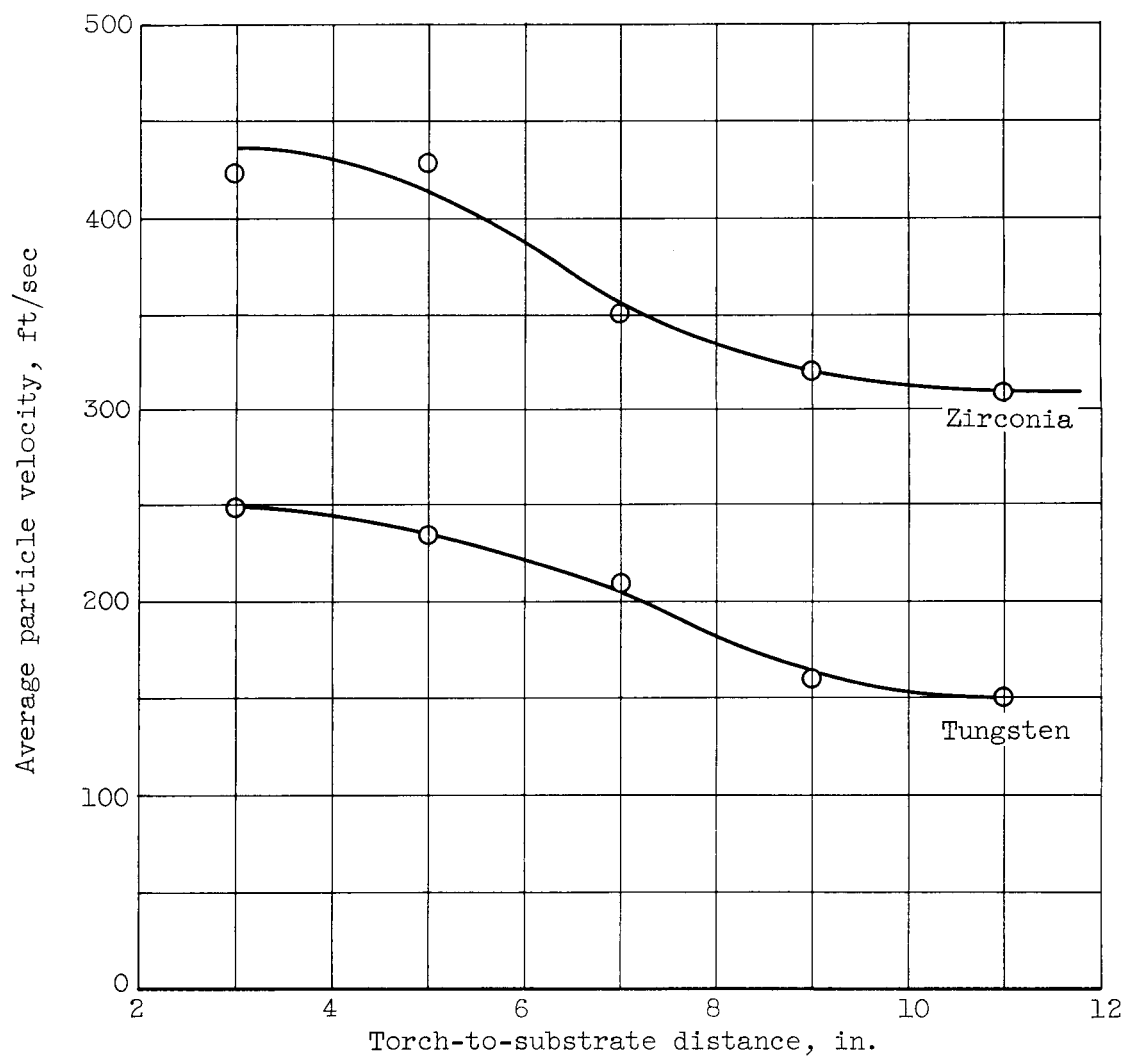


Figure 1. - Variation of average particle velocity with torch-to-substrate distance.

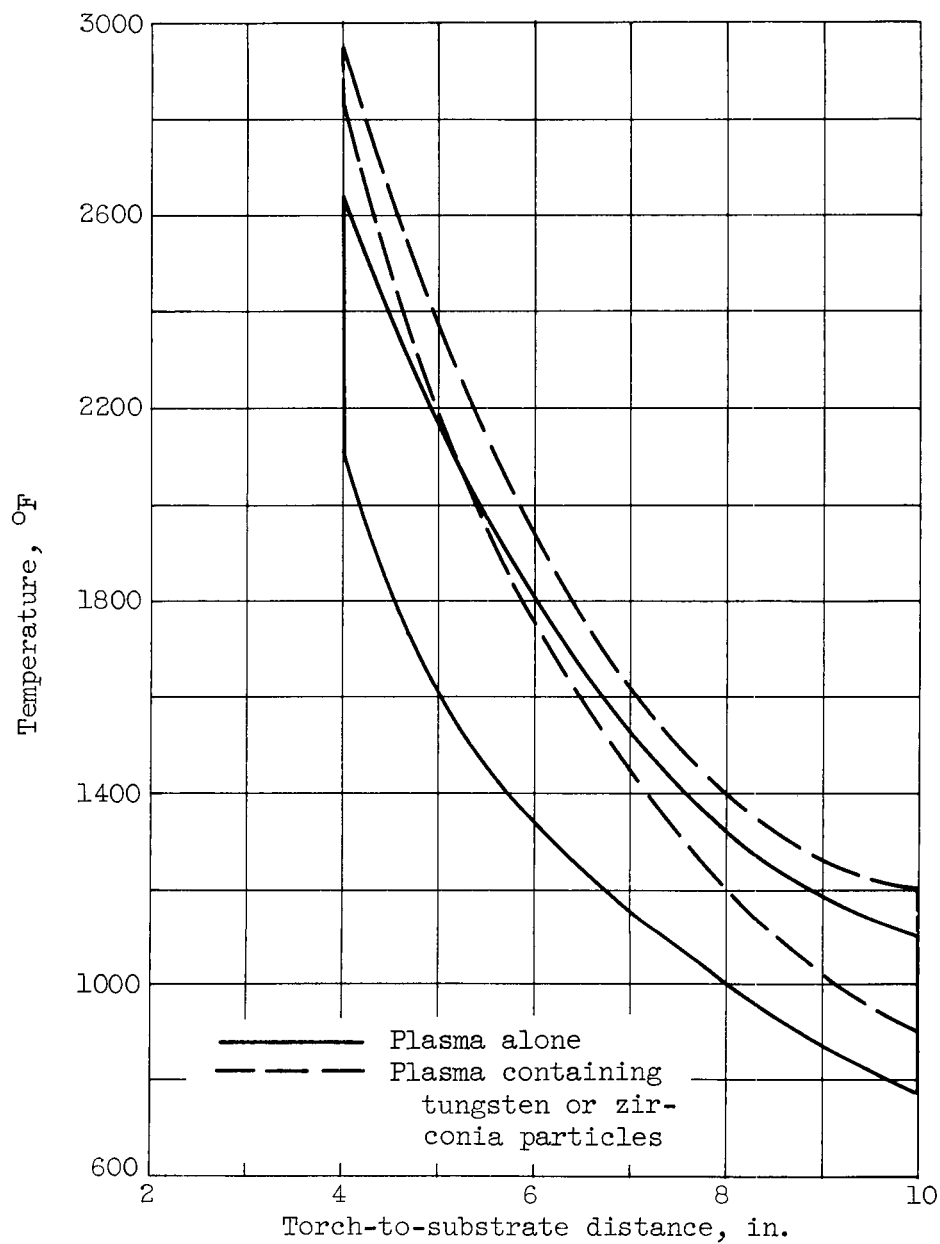


Figure 2. - Temperature variation with torch-to-substrate distance.

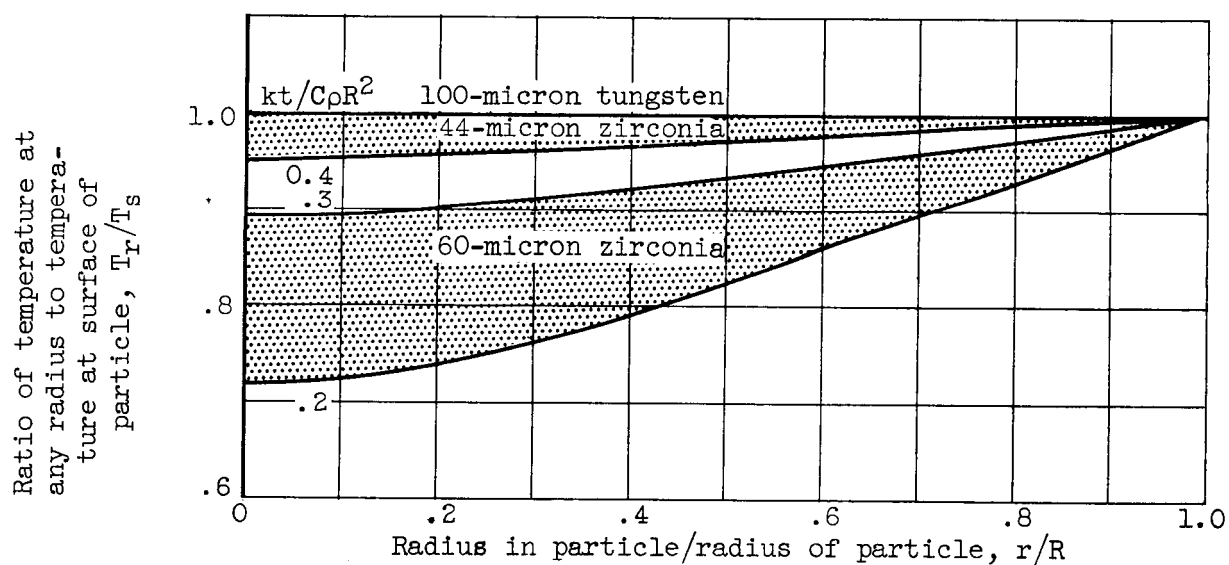


Figure 3. - Temperature distribution at some radius r within a sphere of radius R . Thermal conductivity, k ; residence time, t ; specific heat, C ; density, ρ .

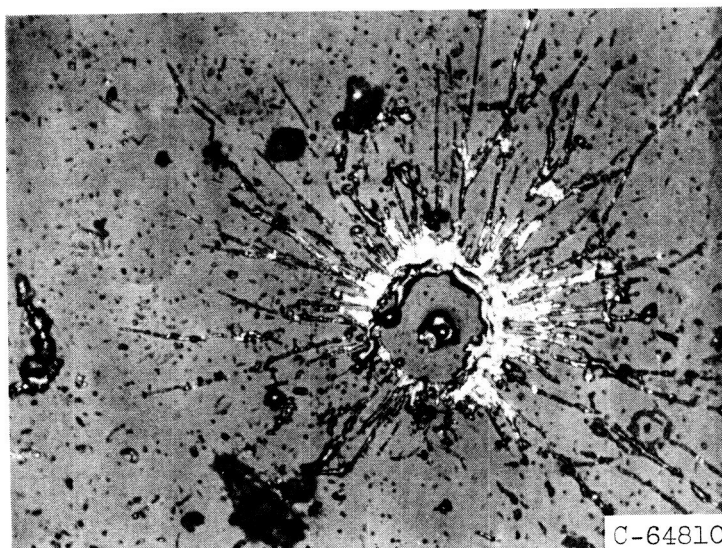


Figure 4. - Zirconia particles on glass substrate. Torch-to-substrate distance, 4 inches. $\times 250$.

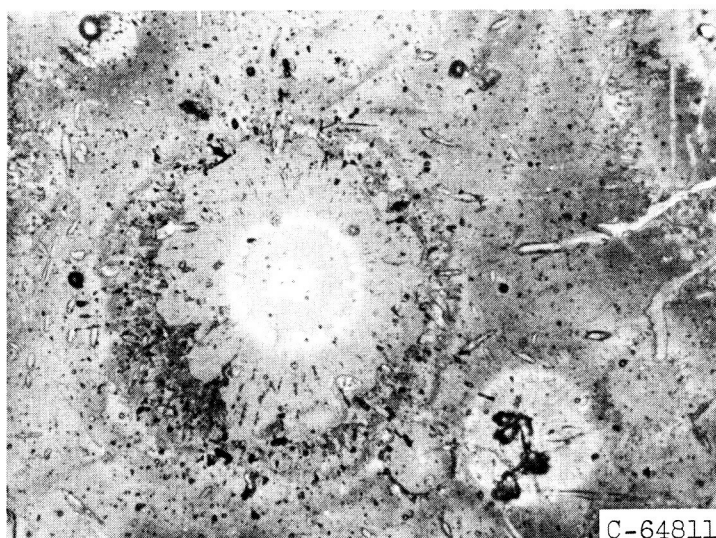
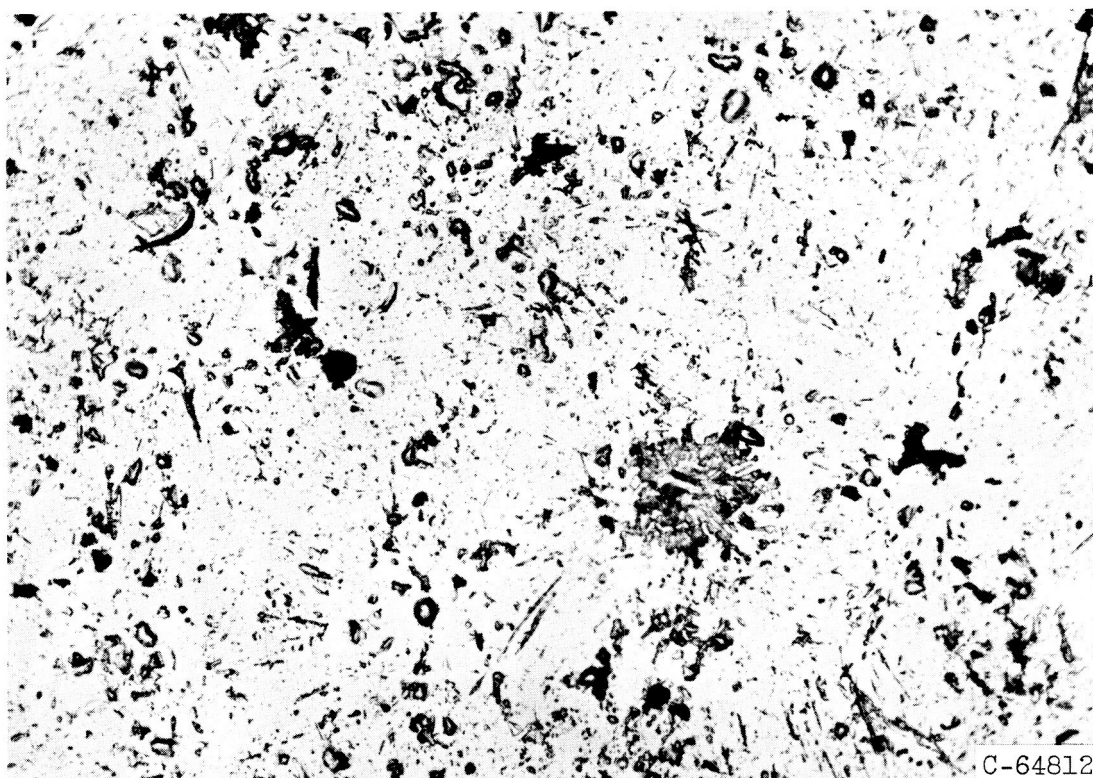


Figure 5. - Tungsten particles on glass substrate. Torch-to-substrate distance, 4 inches. X250.



C-64812

Figure 6. - Zirconia particles on stainless-steel substrate.
Torch-to-substrate distance, 4 inches. $\times 250$.

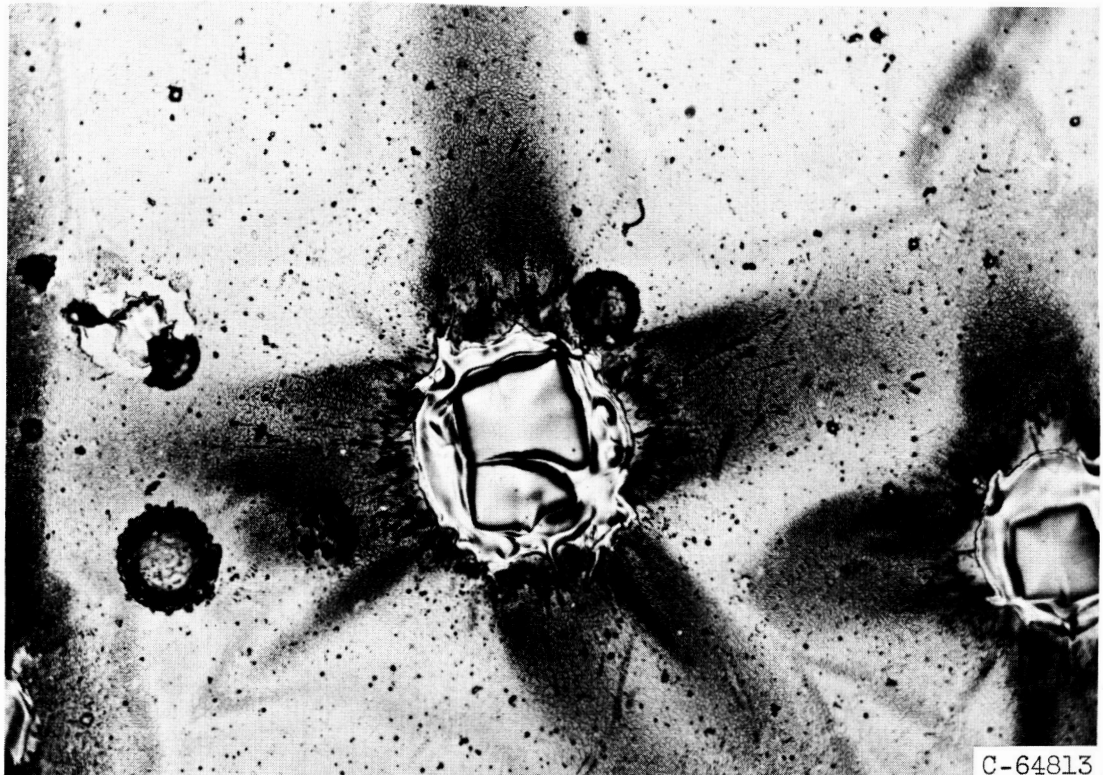


Figure 7. - Tungsten particles on stainless-steel substrate.
Torch-to-substrate distance, 4 inches. X250.

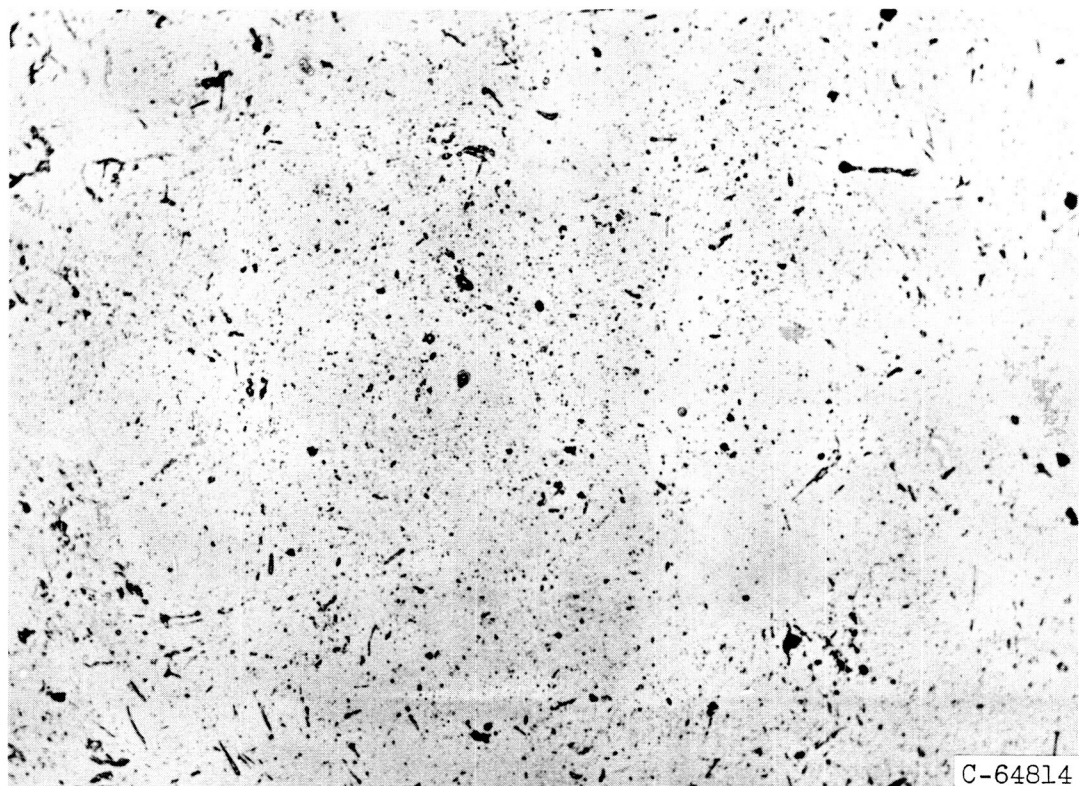


Figure 8. - Fragments of zirconia on tungsten substrate. Torch-to-substrate distance, 4 inches. $\times 250$.

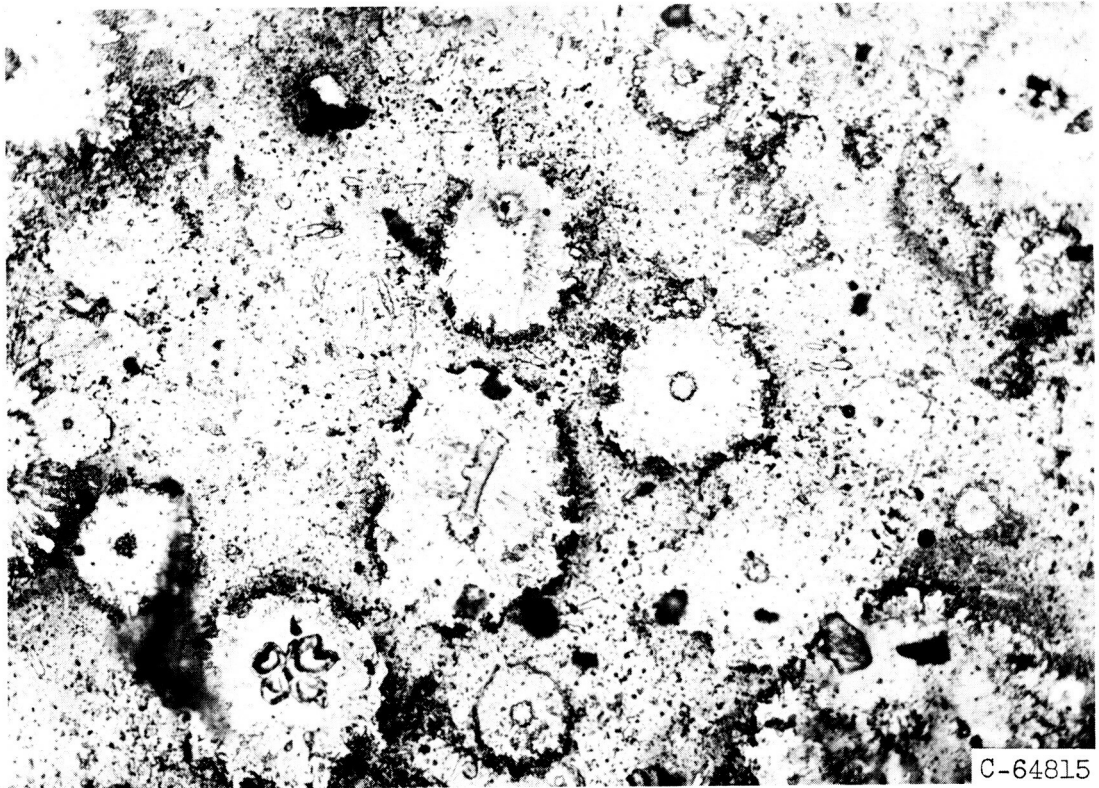


Figure 9. - Areas where tungsten particles collided with, but did not adhere to, tungsten substrate. Torch-to-substrate distance, 4 inches. $\times 250$.

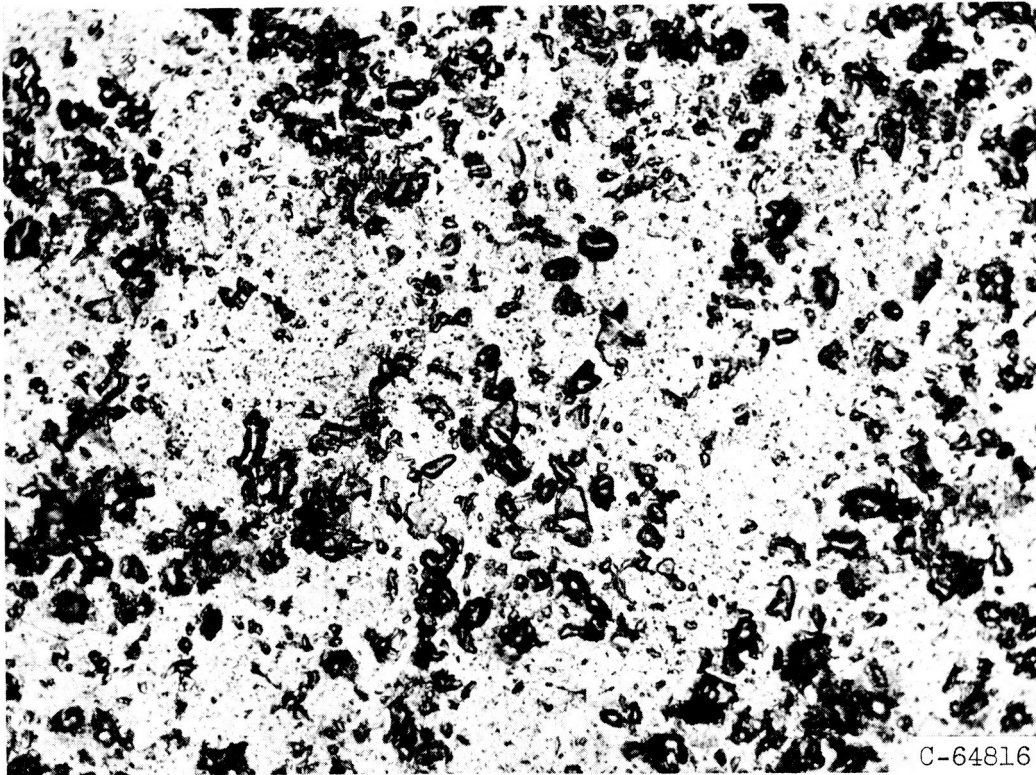
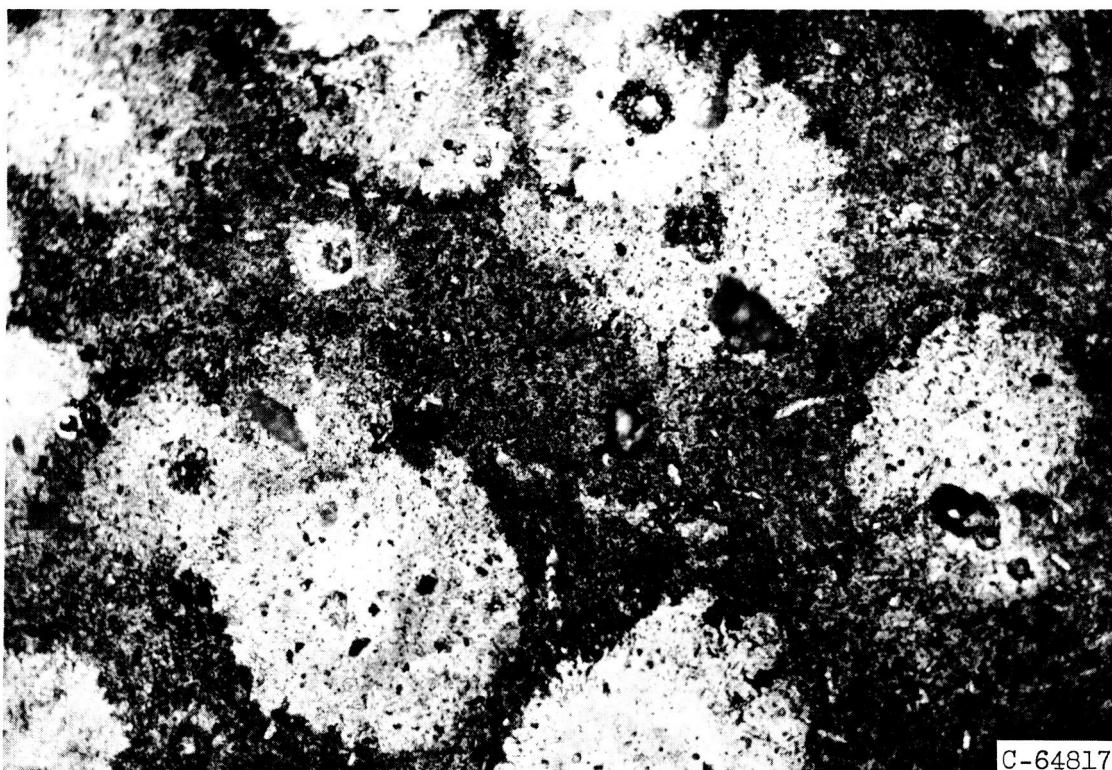


Figure 10. - Pits formed by collisions of zirconia particles with copper substrate. Torch-to-substrate distance, 4 inches. X250.



C-64817

Figure 11. - Areas where tungsten particles collided with, but did not adhere to, copper substrate. Torch-to-substrate distance, 4 inches. $\times 250$.